Available online at www.sciencedirect.com
SCIENCE DIRECT®
International Journal of Pharmaceutics 270 (2004) 263–277
international journal of pharmaceutics
www.elsevier.com/locate/ijpharm

The effect of agitated drying on the morphology of L-threonine (needle-like) crystals

A. Lekhal [a], K.P. Girard [b], M.A. Brown [b], S. Kiang [b], J.G. Khinast [a], B.J. Glasser [a,*]

[a] *Department of Chemical and Biochemical Engineering, Rutgers University, Piscataway, NJ 08854, USA*
[b] *Bristol-Myers Squibb, One Squibb Drive, New Brunswick, NJ 08903-0191, USA*

Received 4 June 2003; received in revised form 21 October 2003; accepted 21 October 2003

Abstract

Experiments have been carried out to study the behavior of L-threonine (needle-like) crystals during agitated drying. For an L-threonine/water system the morphology of the crystals was monitored using light microscopy and image analysis. Analysis of the transient behavior of the crystal size and shape distribution showed that attrition and agglomeration took place simultaneously during the process. The variation of the operating conditions (temperature, agitation and vacuum) revealed that attrition dominated the drying process when the drying rate was low and/or the shear rate was high. For high drying rates and low shear rates, agglomeration became dominant. This study suggests that crystal redissolution had no significant impact on crystal morphology. It was also found that due to their needle-like shape, large L-threonine crystals were very sensitive to attrition. When attrition controlled the drying process, most of the particle size reduction took place below a critical moisture content of 4%. When agglomeration controlled the drying process, most of the crystal size enlargement occurred below a moisture content of 6%.

Keywords: Drying; Crystal; Attrition; Agglomeration; Needle-like; Pharmaceuticals

1. Introduction

Drying, which usually follows crystallization, is one of the last stages in the production of active pharmaceutical ingredients (APIs). While crystallization is a highly controlled process that aims to obtain a product with defined physical properties and chemical purity, the impact of drying on the final crystal properties (crystal shape, size, hardness) is still poorly understood and difficult to predict from first principles. In a recent study on agitated drying of crystals, our group showed (Lekhal et al., 2003) that for particles of cubic shape (i.e., potassium chloride, KCl) it is possible, by using image analysis, to characterize the variation of crystal morphology (size and shape) and to relate the final crystal properties to the operating conditions (temperature, agitation speed and vacuum level). The variation of the crystal size distribution showed that there is a permanent competition between attrition and agglomeration during drying. Furthermore, the analysis of the variation of the average diameter with time and drying conditions revealed that most of the particle size changes due to attrition and agglomeration took place below a critical moisture content of 2%. Above this critical moisture content the liquid solvent acts as a lubricant preventing crystal attrition and the formation of strong agglomerates.

* Corresponding author. Tel.: +1-732-445-4243; fax: +1-732-445-2421.
E-mail address: bglasser@sol.rutgers.edu (B.J. Glasser).

0378-5173/$ – see front matter © 2003 Elsevier B.V. All rights reserved.
doi:10.1016/j.ijpharm.2003.10.022

Nomenclature

d	crystal diameter, μm
$d_{initial}$	initial average diameter, μm
d_{final}	final average diameter, μm
N	agitation speed, rpm
N_{REV}	number of revolutions
P	total pressure inside the drying chamber, atm or Torr
R	drying rate, gram water per gram wet solid/min
t	drying time, min
T	temperature, °C
X	moisture content, gram water per gram wet solid
$X_{initial}$	initial moisture content, gram water per gram wet solid

In the pharmaceutical industry, crystal morphologies can vary widely (e.g., needle-like, plate-like) and their behavior during drying can differ from that of KCl. In particular, it is of interest to examine if a critical moisture content exists for other materials. In addition, if a critical moisture content is indeed a general feature, it can be expected that its value will be a function of the mechanical properties of the material and the crystal morphology. Moreover, it is not clear if there exists a single critical moisture content that applies to both attrition and agglomeration. In this investigation, we use image analysis to characterize needle-like L-threonine crystals and to quantify their behavior during agitated drying. The main objective of this paper is to experimentally examine if crystals of different physical properties (morphology and hardness) exhibit similar behavior under the same drying conditions. In such a case, one would be able to state that the physical phenomena of attrition and agglomeration are independent of particle morphology and agitated drying of crystals becomes more predictable. If dissimilar behaviors are observed, the discrepancies can potentially be explained based on the physical properties and crystal morphology of each material.

During agitated drying, attrition and agglomeration are influenced by the state of the system determined by the moisture level of the wet crystals. As the moisture content decreases during drying, the bed of crystals can exist in a number of different states of liquid saturation (Papadakis and Bahu, 1992). These states were first described by Newitt and Conway-Jones (1958) for wet granulation. In many cases, the initial state for drying corresponds to the capillary state where the voids between particles are saturated with the liquid solvent. As the moisture content decreases, the space between crystals becomes partially filled with the liquid solvent. This state is known as the funicular state. At the end of drying, the moisture content is very low and the crystals enter the pendular state, where they are held together by liquid bridges at their contact points. In the literature most studies dealing with attrition and agglomeration are related to wet agglomeration (Iveson et al., 2001a,b; Abberger et al., 2002; Betz et al., 2003; Rambali et al., 2003).

In an agitated drying process, attrition can lead to the generation of dusty fines. The fines can increase the bulk density of a light product, but they can also be a nuisance and a hazard in the collection of the product (e.g., dust explosion) (Keey, 1992). Also, due to the poor flowability of fines, attrition can seriously impact the subsequent blending stage (when mixed with excipients) and the final tableting process. Crystal size reduction takes place as a result of particles colliding with one another or with the agitator (Bemrose and Bridgwater, 1987; Keey, 1992; Neil and Bridgwater, 1994; Mazzarotta et al., 1996). It can also take place due to stresses induced by temperature or pressure changes inside the drying chamber (Kowalski et al., 2000). Several experimental techniques have been used to identify crystal attrition during drying. When studying the drying of KCl in an agitated unit, Lekhal et al. (2003) used light microscopy to track the crystal size reduction. They found that attrition takes place mainly at low drying rates and/or at high agitation speeds. In wet granulation studies, Vonk et al. (1997), Pearson et al. (1998) and Ramaker et al. (1998) used colored tracer granules. Some of the tracer granules were broken leading to the formation of small fragments. It was observed that larger tracer granules (>1 mm) were more likely to break than small ones. Attrition is affected by the particle properties (size, shape, hardness) and the characteristics of the environment (drying time, shear rate, temperature, pressure, moisture content, etc.). Many attrition studies have shown that the attrition rate is a strong function of the particle shape (Gahn et al., 1996; Schaefer

and Mathiesen, 1996). In particular, it has been found that nearly spherical particles are less prone to attrition or breakage (Bemrose and Bridgwater, 1987). It can be expected that for a given material hardness, a crystal with a cubic shape will show more resistance to attrition than particles with a needle-like shape.

During a drying process agglomeration can produce very large particles. Large agglomerates are usually undesirable due to their low dissolution rate, which may affect a drug's bioavailability. Crystal size enlargement is mostly due to wet crystals coming into contact. Whether or not a collision between two or more crystals results in a permanent bond depends on a wide range of factors, including the mechanical properties and morphology (size and shape) of the crystals (Iveson et al., 2001a). Crystals are held together by liquid bridges due to capillary and viscous forces. These forces keep them from moving apart. In the case of low viscosity solvents, such as water, capillary forces are dominant. Other types of interparticle forces, which can lead to crystal agglomeration, such as electrostatic forces or van der Waals forces, are insignificant in wet systems where particles are larger than 10 μm (Rumpf, 1962). Agglomeration is a strong function of the crystal properties and morphology. Schaefer (1996, 2001) showed that interlocking between plate-like or needle-like crystals produces agglomerates with low strength. Schaefer (1996) also showed that a mixture of needle-like or plate-like crystals and spherical ones generates stronger agglomerates. The strength of the agglomerates is further increased if crystals of irregular shape are used (Schaefer, 2001).

From the above discussion, it becomes clear that during drying, attrition and agglomeration depend on the drying conditions (temperature, shear rate, vacuum, moisture content) as well as on the mechanical properties and morphology of the solid material (size, shape, hardness). The development of a fundamental understanding of these two phenomena is therefore necessary for any rational design and scale-up of industrial dryers. In this work, an experimental procedure is used to characterize the morphology of L-threonine crystals during agitated drying. The paper is organized as follows: in Section 2 the sampling and image analysis procedures used to characterize the solid material are described. The main results are summarized in Section 3, where the impact of the drying conditions (temperature, shear rate and vacuum) on the drying performances and crystal morphology is presented. A comparison between KCl and L-threonine during agitated drying is also provided in this section. Section 4 provides a summary and conclusions.

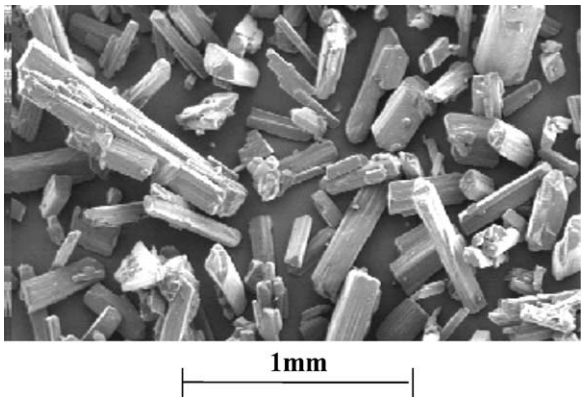

Fig. 1. SEM photograph of L-threonine crystals.

2. Experimental procedure

2.1. Materials and methods

Experiments were carried out in a 800 ml glass reactor equipped with a double envelope, through which a fluid can circulate at constant temperature. The fluid temperature was controlled with a fluid bath. The wet crystals were agitated with a four-blade impeller (Pitched-blade Turbine). Each blade has an angle of 45° with respect to the bottom of the dryer. The agitation speed was varied from 10 to 50 rpm. A vacuum pump was used to maintain a constant pressure inside the dryer. The experimental setup used for this work is described in detail by Lekhal et al. (2003). The material chosen for this study was L-threonine (obtained from Aldrich, Milwaukee, Wisconsin). The choice of this compound is motivated by the fact that the crystals have a needle-like shape (Fig. 1). Several pharmaceutical compounds fall in this category. Moreover, L-threonine does not have any hydrate or solvate forms, which are known to complicate the analysis of the drying process. In order to reduce the variability of the initial conditions, the wet crystals were prepared using a consistent procedure: 60 g of L-threonine (bone dry) were mixed with 25 g of deionized

water in order to evenly distribute the liquid. The wet cake obtained by this operation was filtered under vacuum for 2 min. The filtration time was kept the same for all the experiments in order to obtain similar initial moisture content. We found that under these conditions, the initial moisture content was between 15 and 20%. During drying, samples were taken to determine the variation of the moisture content in the bed and to study the changes in the crystal size and shape distribution. The moisture content was measured using a thermogravimetric moisture analyzer (Sartorius MA50, Sartorius, New York), which has an accuracy of 0.2%. Drying rates were obtained by computing the time derivative of the moisture content curve. For the moisture content analysis, the preliminary results showed that the accuracy of the analysis was drastically improved by increasing the number of samples (Lekhal et al., 2003). In particular, we found that four samples gave sufficiently consistent results, when the samples were taken from different locations in the drying chamber and mixed before the analysis. In order to improve the reproducibility of the samples, a whole segment of the bed was removed in each case using a core sampler with a 5 mm inner diameter.

2.2. Image analysis

Light microscopy pictures of the crystals were captured by a digital camera and subsequently analyzed by the image analysis software 'IMAGE-PRO' (see Lekhal et al., 2003). The average size and shape of each crystal were used to determine the crystal size and shape distributions. The average crystal size of a single crystal was defined as the average length of the distance measured at two degree intervals joining two outline points passing through the center of gravity of the crystal. The shape of the crystals was characterized by the ratio between the height and the width of a box bounding the crystal, where the height of the box is parallel to the largest diameter passing through the center. This parameter will be referred to as the aspect ratio in the rest of the paper.

Preliminary tests showed that when the moisture content was higher than 5%, it was difficult to disperse the crystals consistently on a microscope slide due to cohesive forces. Similar behavior was obtained with KCl. In order to overcome this problem, each sample was mixed with a liquid anti-solvent. A variety of organic and inorganic liquids were tested, and ethyl ether gave the best results (the crystals were insoluble and easily dispersed in ethyl ether). The crystals were gently dispersed in the solvent in order to prevent any changes of the crystal habit. It was observed that when the particle–particle binding forces are weak, the agglomerates disintegrated by themselves, without any agitation, upon contact with the anti-solvent. This allowed discrimination between weak and strong (permanent) agglomerates.

As was observed for the moisture content measurements, the selection of representative samples was also crucial for the image analysis procedure. For each analysis, two samples were taken at the same time from two different locations in the dryer. The samples used for the image analysis were different from the samples used for the moisture content measurements. Two different statistical tests were performed, i.e., one for the average size of the particles and one for the size distribution. For each test about 500 crystals were analyzed. For each sample, the crystal size distribution is given in term of number fraction. The two samples were considered as representative if the difference between both the means and standard deviations were less than 10%. In general, it was found that the standard deviations criterion was more difficult to meet. Finally, it is important to note that the total mass of samples required for the moisture and image analysis did not exceed 10% of the initial mass in the experiment.

3. Results

In Fig. 2a and b two examples of the variation of the measured moisture content, X, and the computed drying rate, R, are plotted. (R is the time derivative of the moisture content X). In the first case (Fig. 2a), the initial moisture content is 14%, while the temperature, agitation speed and pressure are kept constant at 70 °C, 50 rpm and 1 atmosphere respectively. As the drying time advances, the moisture content continuously decreases to reach a value of 0.4%. The end point of the drying was therefore taken to be the first point in time where the moisture content reaches this value. The variation of the drying rate for this particular case reveals the existence of three drying stages: (1) a preheating period, in which part of the energy

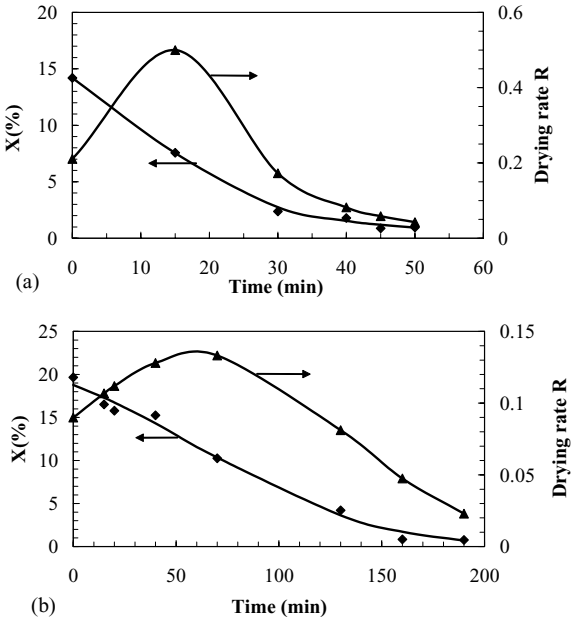

Fig. 2. Changes in moisture content (%) and drying rate during drying process. The drying rate R is given in gram of moisture per gram of wet solid per minute (a) $T = 70\,^{\circ}\mathrm{C}$, $N = 50\,\mathrm{rpm}$, $P = 1\,\mathrm{atm}$, (b) $T = 30\,^{\circ}\mathrm{C}$, $N = 50\,\mathrm{rpm}$, $P = 1\,\mathrm{atm}$.

input is used to evaporate the liquid solvent and warm up the wet crystals, (2) a very short constant rate period, where the rate passes through a maximum, and (3) a falling rate period in which the rate constantly decreases with time. This last stage is controlled by the moisture transport inside the bed. In Fig. 2b, the temperature was lowered to 30 °C and the initial moisture was 20%. The pressure and agitation speed in the dryer remained constant. Decreasing the temperature from 70 to 30 °C reduces the heat transfer rate between the wall and the bed of crystals, which results in a longer drying time. This also explains the lower drying rate at the beginning of the process. It is important to note that, unlike KCl, it was found that L-threonine can easily be mixed inside the dryer at high moisture content. Such observations suggest that the cohesive forces created by the presence of the solvent are less important in this case. This may be due to the fact that the capillary forces are considerably reduced when needle-like crystals are involved (Schaefer, 1996, 2001).

In Fig. 3, the variation of the average particle diameter with time is plotted for the drying conditions presented in Fig. 2b. For each sample, the average

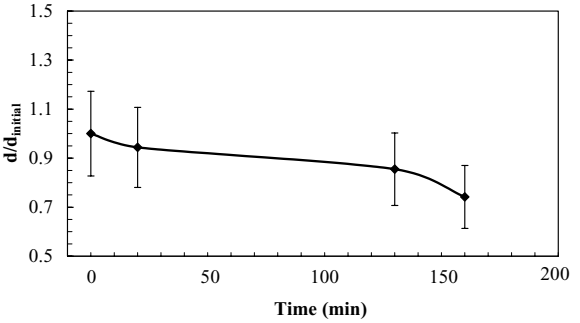

Fig. 3. Variation of average diameter with drying time. $T = 30\,^{\circ}\mathrm{C}$, $N = 50\,\mathrm{rpm}$, $P = 1\,\mathrm{atm}$.

diameter is divided by the initial average diameter. It can be seen that under these conditions, the average diameter decreases with time. At the beginning of drying, when the moisture content is still high, the size reduction is less pronounced (the crystal size decreases by 15% after more than two hours). Most of the attrition takes place when the moisture content is below a value of 4%. The predominance of attrition during the late stages of drying may be due to the fact that at high moisture content crystal-crystal collisions are less frequent because the liquid film between particles has to drain before these collision can occur. The solvent therefore acts as a lubricant (Lekhal et al., 2003). In this work, the continuous crystal attrition or their sudden breakage into smaller fragments are described under the general term attrition. Some very fine crystals were also formed below a moisture content of 2% as shown in Fig. 4a. Such behavior was not reported for potassium chloride. Since, it was important to determine if the dusty fines can be analyzed by optical microscopy, the dusty fines were analyzed by Scanning Electron Microscope (SEM), and it was found that the crystal size for the smallest particles is around 10 μm (Fig. 4b), which is within the detectable range of an optical microscope.

In order to understand the mechanisms by which the particle size reduction takes place for L-threonine crystals, the variation of the crystal size (average diameter) and shape (aspect ratio) distributions with time were analyzed. Fig. 5a shows that the initial crystal size distribution was wide. At an intermediate time, it had only slightly changed (Fig. 5b) with the fraction of large (larger than 400 μm) and small crystals (smaller than 120 μm) being decreased. This trend suggests that

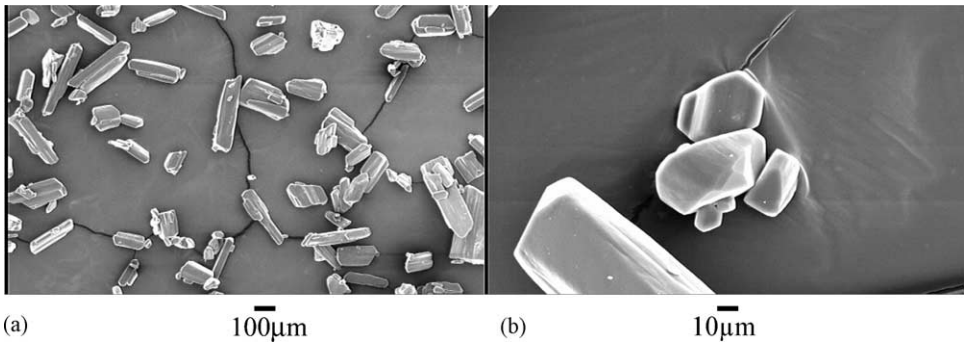

Fig. 4. SEM photographs of small L-threonine crystals when the moisture content is below 2%.

the large crystals were subject to attrition, while most likely the small ones formed agglomerates. Redissolution of the small crystals at this temperature was not likely to have occurred, mainly because the solubility of L-threonine in water is very low at this temperature (5 g/l). The net effect of attrition and agglomeration resulted in a larger fraction of crystals with intermediate size (around 240 μm). At the end of drying (Fig. 5c), the process was dominated by attrition and the fraction of fines was considerably increased, although the final crystal size distribution remained fairly broad. If a smaller average diameter was required for subsequent operations, the drying could be continued beyond the end point defined in this work. This has to be done with some care, since the formation of a dusty material has been observed at very low moisture content.

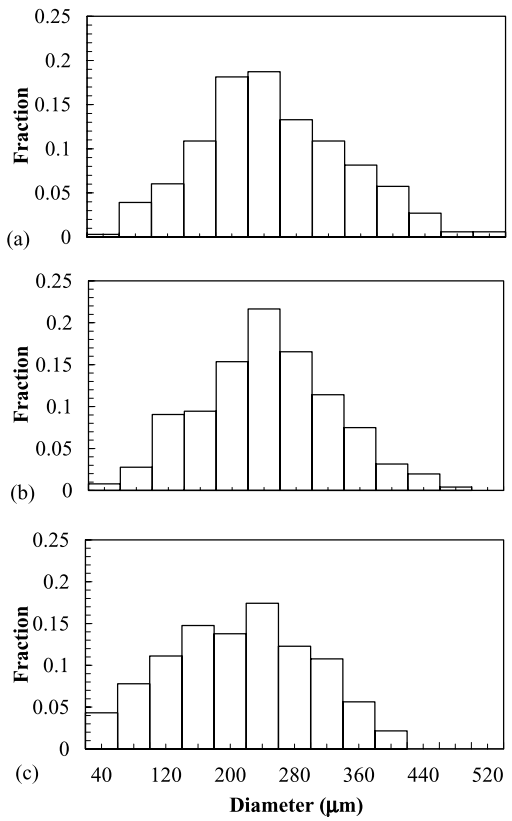

Fig. 5. Variation of particle size distribution. $T = 30\,^{\circ}C$, $N = 50\,rpm$, $P = 1\,atm$. (a) $t = 0\,min$, (b) $t = 20\,min$, (c) t=160 min.

The variation of the shape distribution is shown in Fig. 6. For this particular case, there was initially a large proportion of crystals with an aspect ratio larger than 4. This fraction was reduced at an intermediate time (Fig. 6b), clearly indicating that the crystals with a large aspect ratio were preferentially broken at the beginning of the drying. By comparison with the data from Fig. 5b, one can identify this class of crystals as being those with larger average diameters. Fig. 6b also shows that the fraction of crystals with an aspect ratio close to 1 increased due to attrition. At the end of the drying, the distribution was further shifted towards 1, confirming a strong attrition effect at the late stages of drying, even though a fairly high fraction of "long" crystals still existed. It is important to note that it is very difficult to detect crystal agglomeration by analyzing the particle shape distribution. However, from image analysis, two main modes of crystal agglomeration have been identified for L-threonine crystals. In Fig. 7a, it can be seen that two crystals can agglomerate along their main axis to at the end form a longer agglomerate. Therefore, these two crystals were replaced by a single one with a higher aspect ratio.

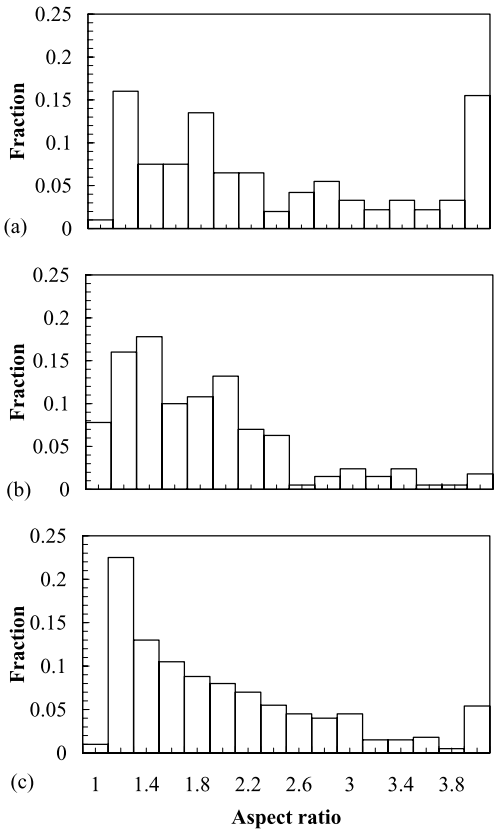

Fig. 6. Variation of particle shape distribution. $T = 30\,^{\circ}C$, $N = 50\,rpm$, $P = 1\,atm$. (a) $t = 0\,min$, (b) $t = 20\,min$, (c) $t = 160\,min$.

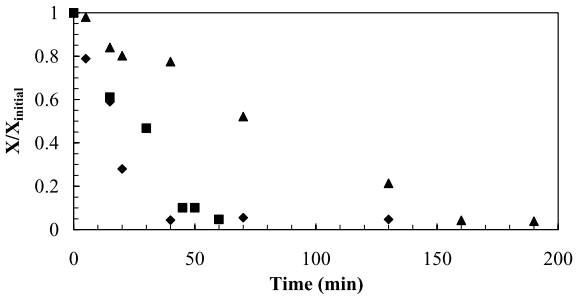

Fig. 8. Effect of temperature on moisture content (%) during drying. $N = 50\,rpm$, $P = 1\,atm$, (▲) $T = 30\,^{\circ}C$, (■) T=50 °C, (◆) $T = 70\,^{\circ}C$.

Fig. 7b showed that two or more crystals could stick to each other on the side to form agglomerates that could potentially have smaller aspect ratio. The image analysis of several agglomerated crystals showed that the second mode of agglomeration was the dominant mode.

3.1. Effect of temperature

Fig. 8 shows the variation of the moisture content with time for three different temperatures (30, 50 and 70 °C). The agitation speed and the pressure in the dryer were kept constant at 50 rpm and 1 atmosphere respectively. For each temperature, the moisture content, X, at a given time was divided by the corresponding initial value. An increase of temperature from 30 to 70 °C increased the drying rate through an increase of the heat transfer between the wall and the wet crystals.

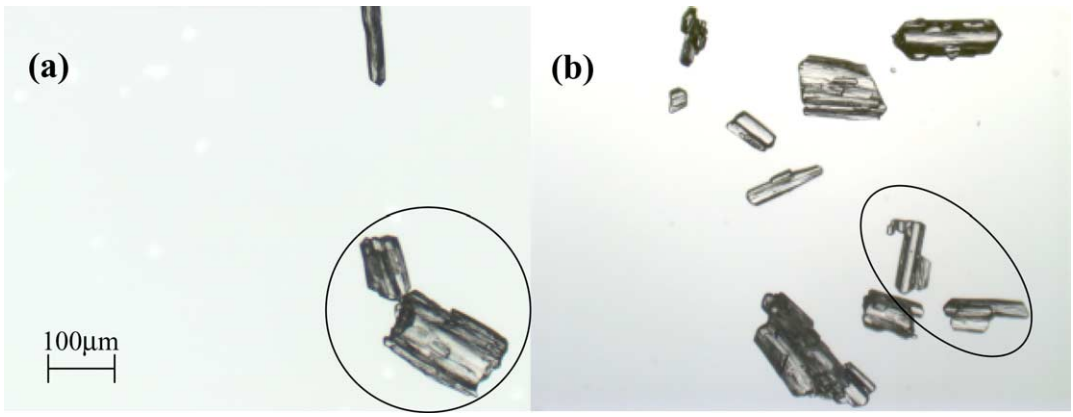

Fig. 7. Different types of crystal agglomeration of L-threonine during agitated drying.

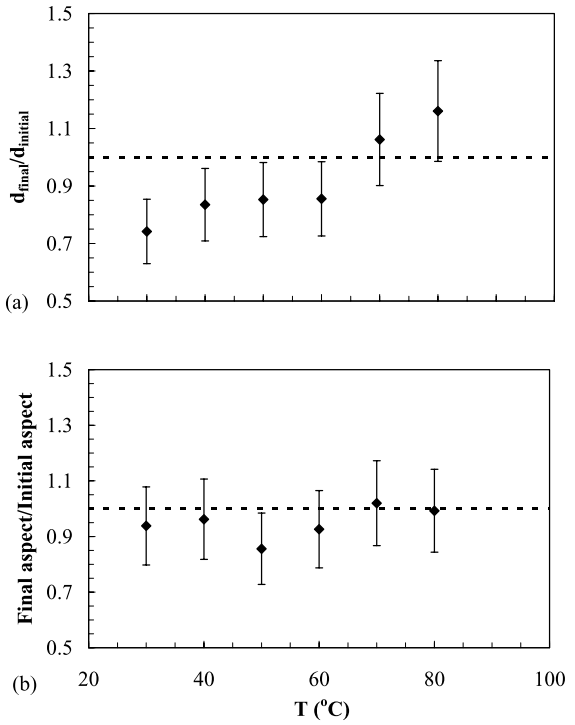

Fig. 9. Effect of temperature on: (a) final average diameter, (b) aspect ratio, $N = 50$ rpm, $P = 1$ atm.

It can be seen that this trend was more pronounced between 30 °C and 50 °C, while there was a smaller difference between 50 and 70 °C. At low temperature (30 °C), the evaporation of the solvent was low and the mixing of the particles, which remained wet for a long period of time, was affected by the cohesive forces due to capillary forces. At 50 and 70 °C, the solvent evaporation was faster and the moisture content dropped very quickly.

The variation of the final average diameter with temperature is plotted in Fig. 9a. In order to take into consideration the variability of the initial particle size distribution for each experiment, the final average diameter was divided by the corresponding initial average diameter. Again, the end point was chosen as the first time where a moisture content of 0.4% was reached. Fig. 9a shows that the final average diameter increased slightly when the temperature was increased from 30 to 40 °C (even though the change was within the experimental error) and it remained fairly constant when the temperature was between 40 and 60 °C. A clear diameter increase was obtained at temperatures of 70–80 °C. An analysis of the variation of the crystal size distribution with time for temperatures between 30 and 60 °C showed that most of the particle size reduction took place when the moisture content was below 4% (as was observed in Fig. 3). As previously stated, when the moisture content was high, the crystal-crystal collisions were less frequent due to the presence of liquid solvent and as a consequence only a small fraction of crystals was attrited. The crystal shape distributions at these temperatures revealed that these crystals were the ones with the larger aspect ratio (as was observed for 30 °C—see Figs. 5 and 6). At 80 °C, it was found that the crystal size distribution was shifted towards a larger crystal size at the end of drying. It was also observed that the fraction of small crystals is reduced, while the fraction of crystals with intermediate size is increased. Some very large crystals were also formed. This is a clear indication that, at high temperature agglomeration dominates drying. High temperatures reduce the drying time and the crystals are less exposed to shear, which is the primary source of attrition. Also, due to a higher solubility, the content of L-threonine in the liquid solution increased, which led to stronger connections between individual crystals. The analysis of the crystal size distribution at 70 °C showed that the crystal size distribution was slightly changed during drying.

Fig. 9b illustrates the variation of the aspect ratio with temperature. For each case, the final average value is divided by the initial average one. At 30 and 40 °C, the aspect ratio was slightly reduced, while at 50 °C it became significantly less than 1, as a consequence of the attrition process that is controlling drying under these conditions. At 70 and 80 °C, the average aspect ratio remains almost unchanged. It is however important to note that overall, the average aspect ratio remains fairly constant.

3.2. Effect of agitation

For many solid materials the drying temperature is limited by the heat sensitivity of the material, and in some cases only low temperatures can be used. In these cases, the variation of the agitation speed is used to enhance the drying rate and reduce the drying time. An increase in agitation speed improves the heat and mass transfer rates by enhancing the mixing of particles

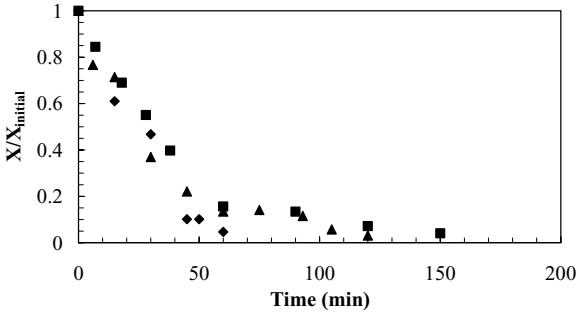

Fig. 10. Effect of agitation speed on moisture content (%). $T = 50\,^{\circ}C$, $P = 1$ atm, (■) $N = 10$ rpm, (▲) $N = 30$ rpm, (◆) $N = 50$ rpm.

inside the dryer (Malhorta and Mujumdar, 1992), and the particle renewal rate at the heat transfer surface. As a result, the rate of evaporation at the free surface is enhanced, leading to high drying rates and shorter drying times. The variation of the moisture content with time in this study is shown for different agitation speeds (10, 30 and 50 rpm) in Fig. 10. The drying temperature and pressure inside the dryer were the same for all the experiments. Fig. 10 showed that under these conditions the effect of agitation speed on the drying performance was negligible, which indicates that the process was not limited by the heat or mass transport, which is an indication that good mixing was achieved in the small drying unit for L-threonine crystals. This will not necessarily be the case for larger drying units such as those employed in manufacturing processes. It is worth noting that good mixing was not obtained for similar agitation rates for the KCl/water system where the agitation rate did have an effect on drying rates and times (Lekhal et al., 2003).

Fig. 11a, which illustrates the variation of the final average diameter with agitation speed, shows that the average diameter constantly decreased with agitation speed. Raising the agitation speed increased the frequency of particle–particle and particle–impeller collisions that can lead to crystal attrition. At low agitation speed (10 rpm), the final crystal size was much larger than the initial one, which indicates that at low shear rates, agglomeration controlled the process. As stated above this shows that the agitation speed can have a drastic impact on the crystal properties, even though its effect on the drying rates was marginal. The shear effect can also be interpreted through the

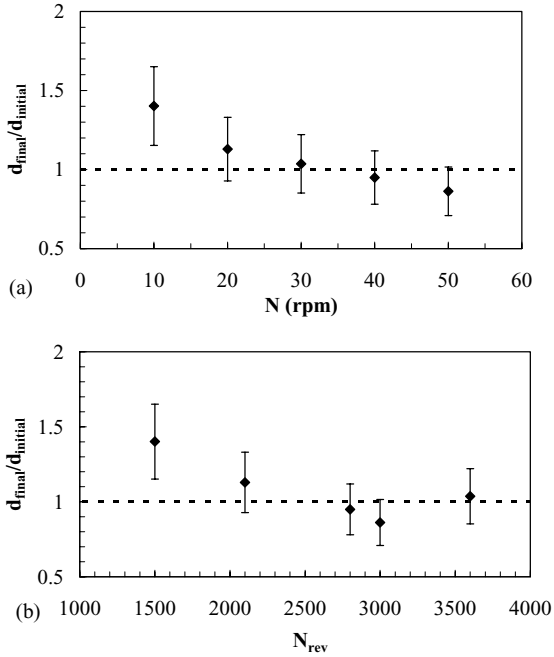

Fig. 11. Effect of (a) agitation and (b) number of revolutions on final average diameter $T = 50\,^{\circ}C$, $P = 1$ atm.

variation of the final average diameter as a function of the total number of revolutions (the number of revolutions is the product of the agitation speed and the drying time). Increasing the number of revolutions from 1500 to 2800 revolutions, increased the probability of particle–impeller and particle–particle collisions, which resulted in a reduced final average diameter (Fig. 11b). However, from 2800 to 3600 revolutions, there was a little change in average particle size. For production scale units (larger units), agitation speed may have a more critical role in defining the crystal properties. Indeed, in such units the shear rate may not be evenly distributed and therefore, near the impeller (high shear zone), attrition would probably dominate, while in other regions of the dryer (low shear zones) agglomeration would control the process. This may lead to a final product with a very broad crystal size distribution.

In order to better understand the behavior of L-threonine crystals during agitated drying, the crystal size distribution is presented for a case where agglomeration is the controlling process. For this purpose, Fig. 12a and b show the crystal size distribution at the

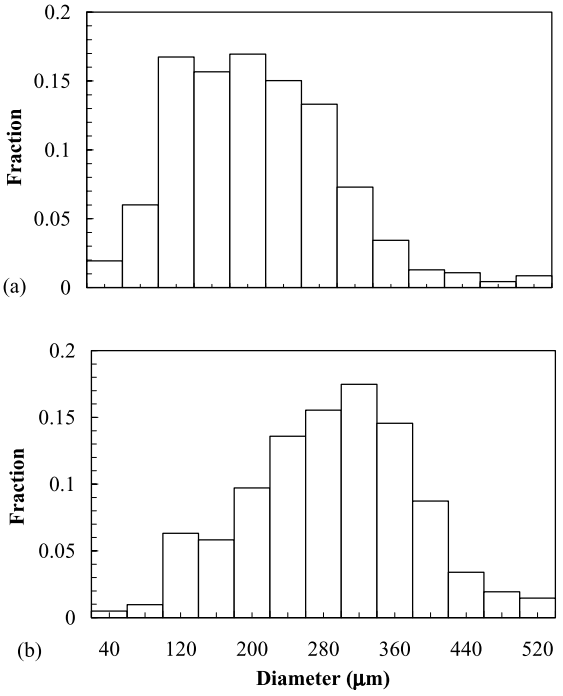

Fig. 12. Variation of particle size distribution. $T = 50\,^{\circ}C$, $N = 10$ rpm, $P = 1$ atm. (a) Initial time, (b) final time.

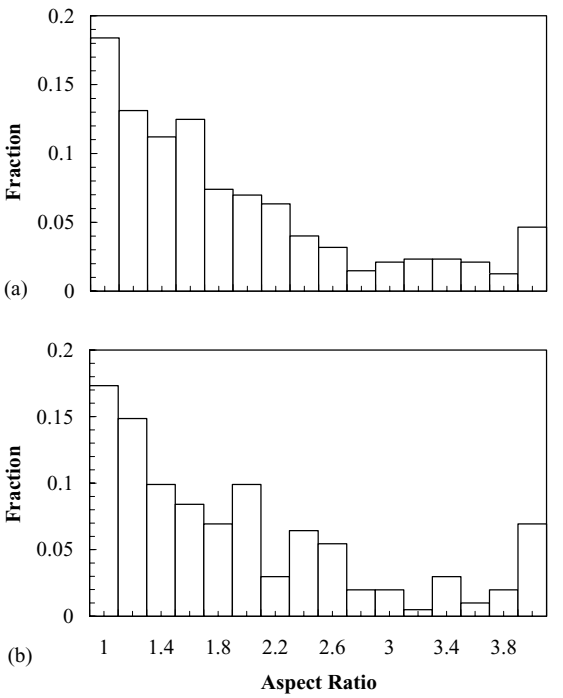

Fig. 13. Variation of particle shape distribution. $T = 50\,^{\circ}C$, $N = 10$ rpm, $P = 1$ atm. (a) Initial time, (b) final time.

beginning and the end of drying for an agitation speed of 10 rpm. It can be seen that initially a large fraction of crystals with a diameter between 80 and 200 μm was present (more than 58% of the population). At the end of the process, the proportion of crystals larger than 280 μm was considerably increased, while the fraction of small crystals (smaller than 200 μm) was reduced. As a result, the size distribution was shifted towards larger diameters. This behavior was also observed for 20 rpm where agglomeration also dominated the process. It can be inferred that due to a low agitation speed the crystals were less exposed to attrition. In addition, at low agitation rates, adjacent crystals could be expected to remain next to each other for longer times, thus increasing the likelihood of agglomerates forming. It is important to note from Fig. 13a and b, which show the crystal shape distribution at the beginning and the end of drying, that it was not possible to see the effect of crystal agglomeration on the shape distribution, as stated previously. Unlike when attrition was dominant (see Fig. 6), the changes between the two distributions were fairly small and a clear trend did not emerge.

Fig. 14a displays the variation of the average aspect ratio with agitation speed. It was found that the aspect ratio was affected by agitation speed, since an increase in the agitation speed generated crystals with small aspect ratio. (It should be noted that the initial average aspect ratio was not the same for all experiments.) The probability of crystal breakage and attrition increased with the agitation speed. As for the average diameter, it is interesting to examine the variation of the aspect ratio with the total number of revolutions. Fig. 14b shows that the average aspect ratio initially decreased with an increase in the number of revolutions. A constant value of the average aspect ratio was, however, reached when the number of revolutions N_{REV} is higher than 2800.

3.3. Effect of pressure

For many porous materials the moisture is either physisorbed or chemically bound to the solid. The

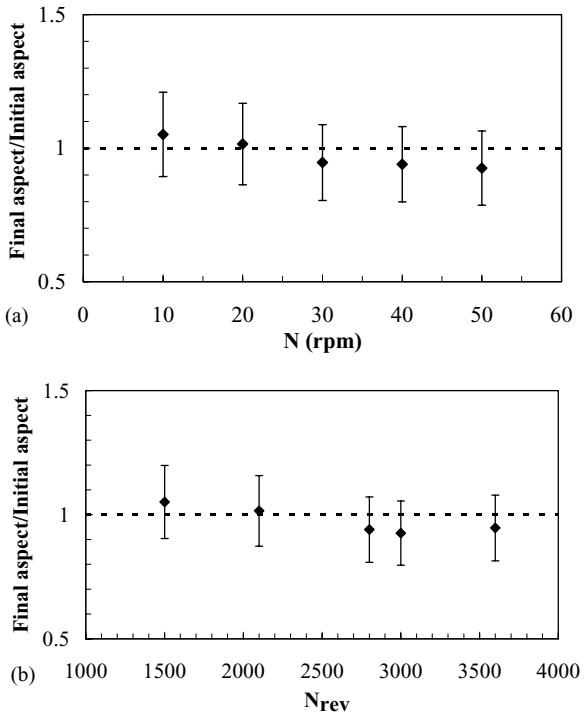

Fig. 14. Effect of (a) agitation and (b) number of revolutions on aspect ratio. $T = 50\,^{\circ}\mathrm{C}$, $P = 1$ atm.

free moisture can easily be evaporated, while the bound moisture can be removed only by severe drying conditions. Such conditions can be obtained at low pressure even for low drying temperatures. In a contact dryer, a decrease of the pressure reduces the heat transfer between the wall and the bed of wet particles. This, however, is compensated by a lower boiling temperature for the liquid solvent. Depending on the solid-liquid system, the drying rate can either increase (Lekhal et al., 2003) or remain nearly unchanged (Heimann and Schlunder, 1988). Fig. 15 shows that for the L-threonine/water system the effect of vacuum was moderate, since the drying time changed only when the pressure was reduced from atmospheric pressure to 200 Torr. Below this value, the solvent was rapidly removed from the system and pressure variations did not have any appreciable effect on the drying performance.

The variation of the average diameter with temperature at different pressures is illustrated in Fig. 16. For the purpose of clarity, the error bars are not shown.

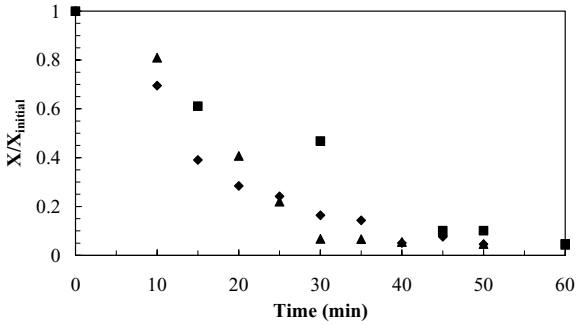

Fig. 15. Effect of pressure on moisture content (%). $T = 50\,^{\circ}\mathrm{C}$, $N = 50$ rpm, (■) $P = 1$ atm, (▲) $P = 200$ Torr, (◆) $P = 80$ Torr.

This figure shows that in general the average diameters obtained at atmospheric drying were smaller than the ones obtained under vacuum. As for the moisture content, the effect of pressure difference was more pronounced between atmospheric pressure and 200 Torr. In most of the cases, the drying process shifted from a regime controlled by attrition (at atmospheric pressure) to a regime dominated by agglomeration (at 200 and 80 Torr). When the drying rate was high, the sensitivity of the results to small experimental variations increased and so did the scatter of the data. Even though there was a significant amount of scatter in the data at low pressure, it can be seen that the drying process was generally controlled by agglomeration. The agglomeration was favored under these conditions because the drying time was low (60 min at atmospheric pressure, 50 °C and 50 rpm; 40 and 30 min at 200 and

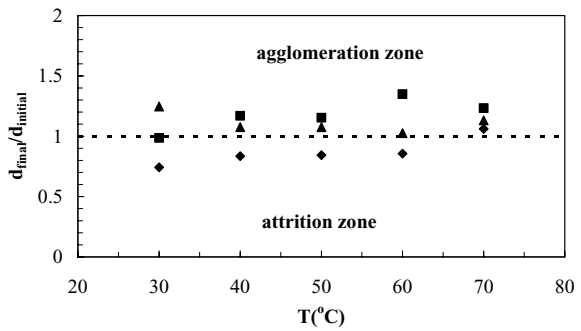

Fig. 16. Effect of pressure on final average diameter. $N = 50$ rpm, (◆) $P = 1$ atm, (■) $P = 200$ Torr, (▲) $P = 80$ Torr.

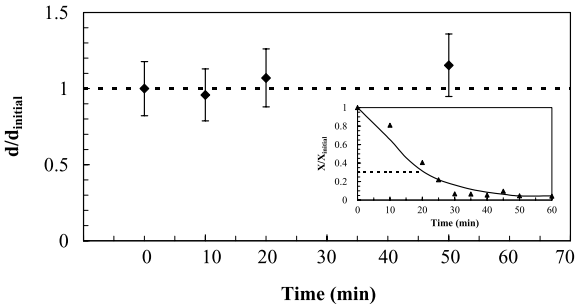

Fig. 17. Variation of average diameter during vacuum drying. $T = 50\,^{\circ}\mathrm{C}$, $N = 50\,\mathrm{rpm}$, $P = 200\,\mathrm{Torr}$, $X_{\mathrm{initial}} = 19.8\%$.

80 Torr, respectively) and the crystals were agitated for less time.

In general, it has been found that agglomeration mainly took place when the moisture content is below 6% (see Fig. 17). In some cases, the agglomeration took place for even lower values of the moisture content. This behavior can be attributed to a wide particle size and shape distribution for L-threonine. Particles of different size and shape can retain different quantities of liquid solvent and therefore the crystals can agglomerate at different levels of moisture content. This may also explain the scattered data obtained at low pressure.

While agglomeration dominated the drying process for vacuum drying at high agitation speed (see Fig. 16) and for atmospheric drying at low agitation speeds (see Fig. 11), there are some important differences. These are highlighted in the analysis of the crystal size distributions. The comparison of initial and final crystal size distribution for a pressure of 200 Torr and temperature and agitation speed of 50 °C and 50 rpm, respectively (see Fig. 18) shows that the fraction of small crystals (smaller than 100 μm) increased. At the same time, the fraction of large crystals was also increased. This trend shows that crystal attrition occurred even though agglomeration was the overall dominating process. However, it is likely that if the material were to be processed beyond the end point as defined in this work, the total average diameter would decrease and the large agglomerates would be attritted. This result also suggests that the agglomeration process is a strong function of the agitation speed.

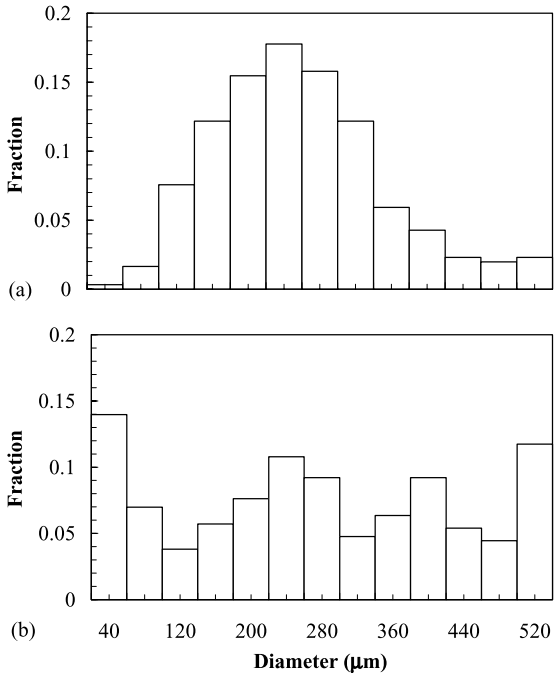

Fig. 18. Variation of particle size distribution. $T = 50\,^{\circ}\mathrm{C}$, $N = 50\,\mathrm{rpm}$, $P = 200\,\mathrm{Torr}$. (a) Initial time, (b) final time.

3.4. Importance of crystal morphology: comparison with KCL

To gain a better understanding of the role that crystal shape can play during agitated drying, it is important at this stage to compare the behavior of L-threonine (needle-like crystals) with potassium chloride (cubic crystals) (Lekhal et al., 2003). For potassium chloride, Lekhal et al. (2003) showed that the contribution of crystal redissolution to crystal size changes can be neglected. Attrition, mainly caused by the rotation of the impeller, dominated drying at low drying rates (low temperature and atmospheric pressure) and high agitation speeds, while agglomeration controlled the crystal size changes at high drying rates (high temperature and/or low pressure). When attrition was the controlling process, the particle size reduction mainly took place when the moisture content was below 2% (the average crystal size was reduced by less than 10%, when the moisture content was above 2%). The critical value is obviously smaller than the one obtained with L-threonine (4%) in this work. This result is not surprising, as it can be understood that elongated

crystals such as L-threonine offer less resistance to attrition and therefore have a higher propensity to break down. The formation of dusty fines when the moisture content reaches 2% also indicates that L-threonine crystals can easily be attrited. Such behavior was not observed with potassium chloride. Another parameter that can also explain the difference in behavior between L-threonine and potassium chloride crystals is the hardness. We have not conducted any quantitative measurement of this parameter, but we have found that L-threonine crystals can be broken just by imposing a pressure with one's hands, which is not the case for the KCl crystals.

The effect of crystal shape on the final crystal properties can also be understood through the variation of the agitation rate. In Figs. 11 and 12, it was shown that the final average diameter and aspect ratio decreased with agitation, while for potassium chloride, Lekhal et al. (2003) reported that only the average diameter decreased. The aspect ratio for KCl was almost unaffected by a change in agitation speed. In fact a crystal with cubic shape has a higher chance to be attrited at the corners (Marrot et al., 2000), which will not necessarily impact the aspect ratio of the particles, while any small fragment removed from a needle-like crystal will reduce the aspect ratio. For L-threonine, the analysis of the shape distribution revealed that crystals with a high aspect ratio were preferentially attrited at the early stage of drying.

The variation of the average diameter at low pressure (when drying is controlled by agglomeration) reveals that agglomeration mainly took place when the moisture content was below 6% for L-threonine. A single value of the critical moisture content for agglomeration was not found. In some cases the majority of the agglomeration took place at a lower value. This is in contrast to what was observed for potassium chloride by Lekhal et al. (2003), where the agglomeration always took place below the same moisture content. Furthermore, the critical value for attrition and agglomeration was the same for KCl. This difference between L-threonine and potassium chloride can be explained by a wider particle size and shape distribution for L-threonine. Particles of different size and shape can retain different quantities of liquid solvent and therefore the crystals can agglomerate at different levels of moisture content. This also may explain the scattered data obtained at low pressure (vacuum drying). In such a case, the agglomeration process is not only controlled by the drying rate and the intensity of agitation, but it is also a strong function of the initial morphology of the crystals (size and shape distribution).

4. Summary and conclusions

In this study, the experimental procedure developed in a recent work by Lekhal et al. (2003) for potassium chloride (cubic crystals), has been applied to characterize and describe the behavior of L-threonine (needle-like crystals) during agitated drying. This procedure allowed the quantification of the impact of drying conditions (temperature, agitation speed and vacuum) on the drying characteristics (drying rate and time) and the final crystals properties (size and shape distribution). Attrition and agglomeration have been shown to compete during the process. Depending on the drying conditions, attrition or agglomeration dominated. While attrition was caused by shear due to the rotation of the impeller, agglomeration was initiated by the liquid bridging caused by the capillary forces (due to the presence of a liquid solution in the system). It was also found that crystal redissolution did not contribute to the crystal size and shape changes. One can expect that crystal redissolution could be significant for hygroscopic materials that have different polymorphic states with a high solubility in the liquid solvent. Further work is needed for hygroscopic materials in order to quantify the impact of redissolution during agitated drying.

The variation of the operating conditions revealed that reducing the pressure in the dryer to a certain extent (from atmospheric pressure to 200 Torr) intensified the agglomeration of the solid material. Under these conditions, the drying rate was enhanced and the drying time was reduced. Therefore, the crystals were less exposed to shear, and the impact of attrition was minimized. An increase of diameter was also observed during atmospheric drying when the temperature was increased. As for the effect of agitation, it was found that the final average diameter was reduced when the agitation speed was increased. In such cases, the particle–particle and particle–impeller collisions became more frequent and the probability of attrition increased. Additionally, the cohesive forces

associated with wet materials were not strong enough to keep the wet agglomerates from separating due to the shape of L-threonine crystals. The variation of the moisture content with time at different agitation speeds showed that the drying characteristics (drying rate and time) were almost insensitive to this parameter. This is perhaps not surprising for our small experimental system where mixing is generally good and thus the heat transfer from the bed to the wall is high. In larger drying units, the shear rate may not be uniformly distributed and the process may be heat transfer limited. Also, a shear rate distribution inside the dryer may lead to the formation of a final product with a broad crystal size distribution. While agglomeration would dominate in low shear zones, attrition would dominate in high shear regions. Further studies with larger units are needed in order to better understand the effect of agitation.

We have observed that most of the changes in crystal size (attrition or agglomeration) occurred below a critical moisture content. This critical value was not the same for attrition and agglomeration (4% for attrition, 6% for agglomeration). In general, it was found that attrition dominated when the drying rate was low and/or the shear rate was high, while agglomeration dominated when the drying rate was high. In a process, where fine particles are undesirable, reducing the shear rate can minimize attrition. However, in large drying units, in order to avoid heat transfer limitations, good mixing is needed. Our results suggest a drying strategy to minimize attrition whereby high agitation rates are maintained until the critical moisture content for attrition is reached. At this point, the agitation rate should be decreased for the final stages of drying. The temperature and pressure in the drying chamber should also be chosen based on the rate of crystal attrition and agglomeration. From the above discussion, it can be concluded that a rational design of the drying process requires a priori knowledge of the critical moisture content for both attrition and agglomeration.

At this stage, it can be seen that several similarities exist between L-threonine and potassium chloride despite a difference in crystal morphology. The differences exhibited during drying can, in most of the cases, be attributed to a difference in morphology (hardness and crystal shape), but further studies with other materials are needed in order to generalize the findings of this work.

Acknowledgements

This work was supported by Bristol-Myers Squibb and the New Jersey Commission on Science and Technology Particle Processing Research Center. We thank Jeannie Chow, Allen Pavlovich, Maria Soares, Juliana Minkah, Viren Thakur, Mark Ignaczack and Joseph Elsabee for assistance.

References

Abberger, T., Seo, A., Schæfer, T., 2002. The effect of droplet size and powder particle size on the mechanisms of nucleation and growth in fluid bed melt agglomeration. Int. J. Pharm. 249, 185–197.

Bemrose, C.R., Bridgwater, J., 1987. A review of attrition and attrition test methods. Powder Technol. 49, 97–126.

Betz, G., Bürgin, P.J., Leuenberger, H., 2003. Power consumption profile analysis and tensile strength measurements during moist agglomeration. Int. J. Pharm. 252, 11–25.

Gahn, C., Krey, J., Mersmann, A., 1996. The effect of impact energy and the shape of crystals on their attrition rate. J. Cryst. Growth 166, 1058–1063.

Heimann, F., Schlunder, E.U., 1988. Vacuum contact drying of mechanically agitated granular beds wetted with a binary mixture. Chem. Eng. Process. 24, 75–91.

Iveson, S.M., Litster, J.D., Hapgood, K., Ennis, B.J., 2001a. Nucleation growth, and breakage phenomena in agitated wet granulation processes: a review. Powder Technol. 117, 3–39.

Iveson, S.M., Wauters, P.A.L., Forrest, S., Litster, J.D., Meesters, G.M.H., Scarlett, B., 2001b. Growth regime map for liquid granules: further development and experimental validation. Powder Technol. 117, 83–97.

Keey, R. B., 1992. Drying of Loose and Particulate Materials. Hemisphere Publishing Corporation, New York.

Kowalski, S.J., Rajewska, K., Rybicki, A., 2000. Destruction of wet materials by drying. Chem. Eng. Sci. 55, 5755–5762.

Lekhal, A., Girard, K.P., Brown, M.M., Kiang, S., Khinast, J.G., Glasser, B.J., 2003. Impact of agitated drying on crystal morphology. Powder Technol. 132, 119–130.

Malhorta, K., Mujumdar, A.S., 1992. Particle flow and contact heat transfer characteristics of stirred granular beds. Drying Technol. 10, 51.

Marrot, B., Pons, M-N., Biscans, B., 2000. Identification of impact attrition mechanisms in solution by morphological analysis. Chem. Eng. J. 79, 123–131.

Mazzarotta, B., Di Cave, S., Bonifazi, G., 1996. Influence of time on crystal attrition in a stirred vessel. AIChE 42, 3554–3558.

Neil, A.U., Bridgwater, J., 1994. Attrition of particulate solids under shear. Powder Technol. 80, 207–219.

Newitt, D.M., Conway-Jones, J.M., 1958. A contribution to the theory and practice of granulation. Trans. Inst. Chem. Eng. 36, 422–441.

Papadakis, S.E., Bahu, R.E., 1992. Sticky issues of drying. Drying Technol. 10, 817–837.

Pearson, J.M.K., Hounslow, M.J., Instone, T., Knight, P.C., 1998. Granulation kinetics: the confounding of particle size and age. In: Proceedings of the World Congress on Particle Technology, Brighton UK, IchemE, Paper #86.

Ramaker, J.S., Jelgersma, M.A., Vonk, P., Kossen, N.W.F., 1998. Scale-down of a high shear pelletisation process: flow profile and growth kinetics. Int. J. Pharm 166, 89–97.

Rambali, B., Baert, L., Massart, D.L., 2003. Scaling up of the fluidized bed granulation process. Int. J. Pharm. 252, 197–206.

Rumpf, H., 1962. In: Knepper, W.A. (Ed.), The Strength of Granules and Agglomerates. AIME, Agglomeration, Interscience, New York, pp. 379–418.

Schaefer, T., Mathiesen, C., 1996. Melt pelletization in a high shear mixer. VII Effect of product temperature. Int. J. Pharm. 134, 105–117.

Schaefer, T., 1996. Melt pelletization in a high shear mixer. X Agglomeration of binary mixtures. Int. J. Pharm. 139, 149–159.

Schaefer, T., 2001. Growth mechanisms in melt agglomeration in high shear mixers. Powder Technol. 117, 68–82.

Vonk, P., Ramaker, J.S., Vromans, H., Kossen, N.W.F., 1997. Growth mechanisms of high shear pelletisation. Int. J. Pharm. 157, 93–102.